Gastrin-Releasing Peptide Phase-Shifts Suprachiasmatic Nuclei Neuronal Rhythms *In Vitro*

Angela J. McArthur,[1] **Andrew N. Coogan,**[3] **Supaporn Ajpru,**[1] **David Sugden,**[1] **Stephany M. Biello,**[2] **and Hugh D. Piggins**[1,3]

[1]*Biomedical Sciences, King's College London, London, United Kingdom SE1 1UL,* [2]*Department of Psychology, University of Glasgow, Glasgow, G12 8QB United Kingdom, and* [3]*School of Biological Sciences, University of Manchester, Manchester, United Kingdom M13 9PT*

The main mammalian circadian pacemaker is located in the suprachiasmatic nuclei (SCN) of the hypothalamus. Gastrin-releasing peptide (GRP) and its receptor (BB_2) are synthesized by rodent SCN neurons, but the role of GRP in circadian rhythm processes is unknown. In this study, we examined the phase-resetting actions of GRP on the electrical activity rhythms of hamster and rat SCN neurons *in vitro*. In both rat and hamster SCN slices, GRP treatment during the day did not alter the time of peak SCN firing. In contrast, GRP application early in the subjective night phase-delayed, whereas similar treatment later in the subjective night phase-advanced the firing rate rhythm in rat and hamster SCN slices. These phase shifts were completely blocked by the selective BB_2 receptor antagonist, [D-Phe[6], Des-Met[14]]-bombesin 6–14 ethylamide. We also investigated the temporal changes in the expression of genes for the BB_1 and BB_2 receptors in the rat SCN using a quantitative competitive RT-PCR protocol. The expression of the genes for both receptors was easily detected, but their expression did not vary over the diurnal cycle. These data show that GRP phase-dependently phase resets the rodent SCN circadian pacemaker *in vitro* apparently via the BB_2 receptor. Because this pattern of phase shifting resembles that of light on rodent behavioral rhythms, these results support the contention that GRP participates in the photic entrainment of the rodent SCN circadian pacemaker.

Key words: gastrin-releasing peptide; bombesin; suprachiasmatic nucleus; circadian rhythms; brain slice; rat; hamster

Daily variation in an organism's physiology and behavior is determined by the interaction between intrinsic circadian pacemakers and recurring environmental cues. In mammals, the dominant circadian pacemaker is located in the suprachiasmatic nuclei (SCN) of the hypothalamus (Meijer and Rietveld, 1989; Ralph et al., 1990). The SCN circadian pacemaker is entrained (synchronized) to the environmental light/dark conditions by photic information conveyed directly to the SCN through the retinohypothalamic tract (RHT) and indirectly via retinally innervated cells of the thalamic intergeniculate leaflet (Harrington, 1997).

A critical research problem in circadian biology is the identification of the neurochemical basis for entrainment of the SCN circadian pacemaker. Converging evidence has demonstrated that glutamate is the main neurotransmitter of the RHT (Colwell and Menaker, 1996; Ebling, 1996; Piggins and Rusak, 1999), whereas neuropeptide Y and GABA are key neurochemicals of the thalamic input to the SCN (Harrington, 1997). Prominent among the many neuropeptides synthesized within SCN cells is the 27 amino acid gastrin-releasing peptide (GRP). Both GRP protein and mRNA have been localized to cells in the retinally innervated ventral SCN by immunohistochemistry and *in situ* hybridization, respectively (Roth et al., 1982; Panula et al., 1984; Mikkelsen et al., 1991; Zoeller et al., 1992). Furthermore, radioligand investigations have shown intense expression of high-affinity GRP binding sites in the rodent SCN (Ladenheim et al., 1990, 1992). *In situ* hybridization studies have reported heavy expression of mRNA for the BB_2 receptor in the rat SCN, and this receptor is believed to mediate the effects of GRP on rodent neurons (Battey and Wada, 1991).

A number of reports indicate that GRP may play a role in the photic entrainment of the SCN circadian pacemaker. GRP-containing neurons receive a direct retinal input, demonstrating that photic information is conveyed directly to these neurons (Tanaka et al., 1997; Aïoun et al., 1998). Light pulses induce immediate early gene expression in GRP-containing SCN neurons (Earnest et al., 1993; Romijn et al., 1996; Aïoun et al., 1998), and levels of GRP and GRP mRNA within the rat SCN are altered by photic conditions (Zoeller et al., 1992; Okamura and Ibata, 1994). However, results from *in vivo* studies are less clear. Albers and colleagues (1991, 1995) found that microinjection of GRP into the SCN region did not significantly alter hamster wheel-running rhythms, whereas other researchers have found that microinjection of GRP phase-dependently evoked phase shifts in hamster behavior rhythms that were comparable in magnitude and direction to those elicited by light pulses (Piggins et al., 1995).

Because the results of behavioral studies on GRP have been inconclusive, in the present study we attempted to define a functional role for this peptide in circadian rhythm processes by examining the effect of GRP on the phase of electrical activity rhythms of rat and hamster SCN neurons *in vitro*. We also investigated the possibility that temporal variation in the expression of GRP receptors in the SCN might underlie the phase dependency of this peptide's actions through a competitive RT-PCR protocol.

MATERIALS AND METHODS

Electrophysiology studies

Rats. Adult male Wistar rats (6–8 weeks of age) purchased from the inbred colony at King's College London and Charles River (Margate, UK) were housed at either King's College London or the University of Manchester. At both sites, the animals were maintained on a 12 hr light/dark environmental lighting cycle with food and water available *ad libitum* for at least 10 d before they were used in experiments. By convention, lights off was defined as zeitgeber time (ZT) 12. Rats were removed from the colony and decapitated under mild halothane anesthesia during the lights-on period only. Coronal brain slices (500 μm thick) were prepared using a Vibroslicer (Campden Instruments, Sileby, UK) and maintained in a Hatton-style

brain slice chamber. The slices were continually perfused with Earle's balanced salt solution (EBSS; Sigma, Poole, UK) supplemented with 24.6 mM glucose, 26.2 mM sodium bicarbonate, and 0.0005% gentamicin (Sigma). The EBSS was adjusted to pH 7.2, warmed to 37°C, saturated with 95% O_2/5% CO_2, and delivered to the slice chamber via peristaltic pump at a flow rate of ~1 ml/min. The slices were allowed to equilibrate for at least 1 hr before any experimental paradigms were initiated.

Drug treatments were administered via bath application. At specific zeitgeber times (ZT6, ZT13, or ZT19), the medium in the dish was replaced with pharmacological agents dissolved in EBSS. After drug application (see below), the slice was perfused continuously with EBSS until the conclusion of the experiment. (1) GRP (Bachem, Saffron Waldon, UK and GenoSys, Cambridge, UK) was dissolved in saline to 10^{-3} M then serially diluted to 10^{-5} to 10^{-11} M in EBSS and applied for 30 min. (2) The BB_2 receptor antagonist, [DPhe^6, Des-Met^{14}]-bombesin 6–14 ethylamide (DPDMBE; Peninsula Laboratories, UK) was dissolved in the same fashion to 10^{-5} M working solution and administered for 45 min, beginning 15 min before the ZT to be tested. (3) In those experiments in which GRP and DPDMBE were concurrently administered for 30 min, a 15 min preincubation with DPDMBE alone was performed.

Glass microelectrodes filled with 2 M NaCl were used to randomly sample single-unit extracellular activity throughout the SCN. Each spontaneously discharging cell was monitored for 4 min to determine its mean firing rate. Cells were grouped into 2 hr bins according to the time of recording, and the data were smoothed by plotting 15 min running averages. Total cell count per experiment ranged from 45 to 98 units, with the duration of recording periods varying from 8–14 hr. Two colleagues who were unaware of slice treatments visually discerned the time of peak, and the phase-shift magnitude was calculated as the difference between the experimental result and the mean time of peak in untreated control slices. Preliminary data indicated that the peak in the firing rate rhythm in SCN slices under control conditions did not vary from rats purchased from King's College London or Charles River and that GRP had similar phase-shifting actions on rat slices from animals housed at either location. Consequently, the data were collapsed into one set for analysis of the phase-resetting actions of GRP.

Hamsters. Male Syrian (*Mesocricetus auratus*) hamsters, 40–60 d old, were purchased from Charles River and divided into two groups that were held in rooms under opposite photoperiods, with both rooms under a light/dark schedule of 14/10 hr. Lights off in the animal room was designated ZT12 by convention. Hypothalamic slices (~400–500 μm thick) containing the SCN were obtained from hamsters in a manner similar to that described above for rat SCN slices, placed in a gas-fluid interface slice chamber (Medical Systems BSC with Haas top), and bathed continuously (1 ml/min) in artificial CSF (ACSF) containing (in mM): 125.2 NaCl, 3.8 KCl, 1.2 KH_2PO_4, 1.8 $CaCl_2$, 1 $MgSO_4$, 24.8 $NaHCO_3$, and 10 glucose. ACSF, pH 7.4, was supplemented with an antibiotic (gentamicin, 0.05 gm/l) and a fungicide (amphotericin, 2 mg/l) and maintained at 34.5°C with warm, humidified 95% O_2/5% CO_2.

Extracellular single-unit activity of hamster SCN cells was detected with glass micropipette electrodes filled with either 2 M NaCl or ACSF, as described above for rats. The average spontaneous firing rate (measured for 3–5 min) and the ZT for each single unit encountered were recorded by an experimenter blind to all treatments. Slices without significant differences across firing rate data, when grouped into 1 hr bins ($p > 0.05$; one-way ANOVA), were not used for further analysis (two hamster slices failed to meet this criterion and were discarded from analysis). If significant differences were found, the data were smoothed by 1 hr running means with a 15 min lag. Total cell counts per experiment ranged from 82 to 134. The time corresponding to the maximum of the smoothed data was used as the time of the peak firing. Drug-induced phase shifts were measured relative to the average time of peak firing of control slices.

Treatments were administered via microdrop and/or bath application at one of three zeitgeber times (ZT6, ZT14, or ZT18). For microdrop application, drugs were warmed to 34.5°C and applied as a 200 nl microdrop to the SCN area. This was done at least 1 hr after slice preparation, using a Hamilton 1 μl syringe. For bath application, the tubing for the perfusion medium was removed from the ACSF and placed in ACSF-containing the pharmacological agent to be tested. The perfusion of this new medium continued for 30 min centered around the ZT of investigation. At the end of the treatment, the perfusion tubing was returned to the ACSF.

GRP (Bachem and GenoSys) were dissolved in ACSF to 10^{-7} M and administered via either the bath or microdrop. The BB_2 receptor antagonist DPDMBE was administered via bath application only. When the antagonist and GRP were administered together, bath application of the antagonist began 15 min before microdrop application of GRP and continued for an additional 15 min.

Competitive quantitative RT-PCR of rat SCN

Male Wistar rats (inbred King's College London strain) were housed under a 12 hr light/dark schedule (lights on at 7 A.M.) with food and water available *ad libitum*; room temperature was 21 ± 1°C. To monitor physiological and behavioral rhythms, a representative sample of rats were implanted with a telemetry probe (VM-FH disk model, ~4.0 gm; Mini-Mitter Co., Sunriver, OR) under halothane anesthesia and housed singly in plastic cages equipped with radiotelemetry equipment (Dataquest III;

Mini-Mitter Co.). Core body temperature and locomotor activity were recorded at 5 min intervals continuously for the 14 d. All animals monitored by telemetry showed tight coupling of core temperature and ambulatory activity rhythms to the 12 hr light/dark cycle.

After the 2 week telemetry monitoring period to verify entrainment, rats were killed at 4 hr intervals corresponding to ZT2, ZT6, ZT10, ZT14, ZT18, and ZT22 (where ZT0 = lights on and ZT12 = lights off; $n = 6$ per ZT) across the day–night cycle. Animals were observed during the dark portion of the cycle using a helmet-mounted infrared viewer (Night Vision Goggles Model MPN-35K-1; Moonlight Products, San Diego, CA). Hypothalamic slices (~500 μm thick) containing the SCN were prepared as described above for the rat neurophysiological studies. Slices were placed on an ice-cooled platform, and the tissue adjacent to the SCN was dissected away under microscopic observation so that virtually all non-SCN tissue was removed. The optic chiasm directly ventral to the SCN was not removed because SCN cells are embedded in this structure. The reduced SCN slice was placed in a nuclease-free microfuge tube and immediately frozen on dry ice. Samples were stored at −70°C until mRNA was isolated. All sample preparations were performed by one of the authors (A.J.M.) to reduce variability between slices.

Isolation of mRNA and reverse transcription

Each reduced SCN slice was sonicated on ice in 200 μl lysis buffer (Tris-HCl 100 mM, pH 8.0, LiCl 500 mM, EDTA 10 mM, lithium dodecylsulfate 0.1%, dithiothreitol 5 mM), and mRNA was isolated using magnetic oligo $(dT)_{25}$ beads (Dynal, Wirral, UK). cDNA was synthesized from each mRNA sample immediately. Oligo$(dT)_{18}$ (1 μg) and random 10-mers (1 μg) were added to the mRNA, and the mixture was heated (70°C; 5 min) to remove secondary RNA structure, then cooled immediately on ice. DTT (20 mM), dATP, dCTP, dTTP, and dGTP (all 0.5 mM; Promega, Southampton, UK), recombinant ribonuclease inhibitor (80 U RNasin, Promega), avian Moloney murine leukemia virus-reverse transcriptase (200 U, MMLV-RT, Promega), and diethyl pyrocarbonate-treated water were added to make the final volume 20 μl, and the mixture was incubated at 37°C for 1 hr, then 42°C for 15 min. MMLV-RT was inactivated (98°C for 3 min), and SCN cDNA was diluted 10-fold in tRNA (10 μg/ml) and stored at −70°C. Pairs of SCN samples from each of the six ZT points were extracted in each batch and then immediately reverse-transcribed using a single master mix of reagents.

Competitive PCR

PCR primers were designed from the sequence of rat BB_1 (GenBank accession number U37058) and BB_2 (U56661) receptors using the PRIME program of the Genetics Computer Group Sequence Analysis Software Package (Devereux et al., 1984). A single BB_1 and BB_2 sense primer (5'-GTW CTG GTG TTT GTG GTG GGC-3') and specific antisense primers (BB_1, 5'-ATT GGA TGG TCT CCG ATC-3'; BB_2, 5'-TGG TGC TCT TGA AGG AGG-3') were used. Competitor BB_1 and BB_2 receptor DNAs (316 and 363 bp, respectively) were made using low-stringency amplification of *Escherichia coli* DNA with the specific primer pairs as described by Uberla et al. (1991). Competitors were cut from a gel and spin column-purified (Qiaquick gel extraction kit; Quiagen Crawley, Sussex, UK). The amount of competitor was measured by comparing its density with known amounts of molecular weight standards (*Hpa*II digest of pBluescript SK$^+$) on an agarose gel stained with ethidium bromide (EtBr, 0.5 μg/ml). The efficiency of PCR amplification of each competitor and target pair was determined by measuring the amount of each produced in a single reaction tube during successive cycles of the exponential phase of amplification. This was done by separating target and competitor PCR products by agarose gel electrophoresis, staining with EtBr, and quantitating bands by densitometry.

Competitive PCR was performed on a thermal cycler (Hybaid Omnigene) in a reaction (20 μl) containing 100 μM of each deoxynucleoside 5'-triphosphate, 0.5 μM of each primer, 1 mM $MgCl_2$, 1 μl of 10-fold diluted SCN cDNA and 1 μl of five twofold dilutions of competitor DNA. Reactions were initiated using a "hot-start" procedure (D'Aquila et al., 1991) by adding 1 U of *Taq* DNA polymerase (Promega, Madison, WI) to each tube. Thermal cycling conditions were as follows: denaturation at 94°C for 1 min, annealing at 56°C for 1 min (BB_1)/58°C for 1 min (BB_2), and 72°C for 2 min for 40 cycles with a final extension of 5 min at 72°C. PCR reaction products were resolved by agarose gel electrophoresis (2.0% w/v) and stained with EtBr. The same master mix containing all reagents, including the appropriate concentration of competitor, was used to assay all samples. Each competitive PCR assay included equal numbers of SCN cDNA samples from each time point. The identity of the amplification product for BB_1 and BB_2 was confirmed by direct sequencing of the purified PCR product on an ABI automated sequencer (courtesy of Department of Molecular Medicine, King's College Hospital London).

Statistical analysis

Statistical significance of the effects of drug treatments on the peak time in firing rate rhythms was tested using one-way or two-way ANOVA, followed by either Dunnett's or Tukey HSD *post hoc* tests, where appropriate. Significance was set at $p < 0.05$, and Bonferonni adjustments were made to α levels when a data set was used in more than one ANOVA. Statistical analyses were performed using Systat 9.0 (SPSS Inc.) on a Pentium PC.
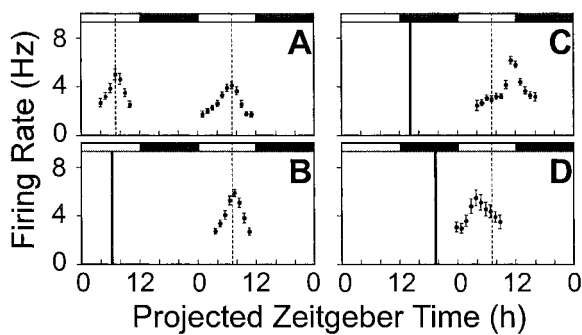
Figure 1. Firing rate rhythms of rat SCN neurons *in vitro* across two projected day–night cycles. *A,* The peak in control untreated slices occurred at projected ZT7.06 on the first day *in vitro* and projected ZT7 of the second day *in vitro.* *B,* Bath-applied GRP (10^{-7} M) (*filled vertical bar*) at ZT6 did not significantly alter the time of peak compared with control slices (*vertical dashed line*). *C,* GRP (10^{-7} M) at ZT13 phase-delayed the peak in this rhythm. *D,* GRP (10^{-7} M) at ZT19, phase-advanced the timing of the peak in this rhythm. In each panel, the *solid dots* represent the smoothed running mean firing rate in spikes per second, and the *vertical bars* are the standard error of that smoothed firing rate mean. *Filled* and *unfilled horizontal bars* depict projected night and day portions, respectively, of the projected 48 hr period.

RESULTS

Electrophysiology: rats

GRP resets the rat SCN clock at early and late subjective night

The action of GRP on the rat SCN circadian pacemaker was assessed by monitoring the time of peak in the endogenous ensemble firing rate rhythm in SCN neurons. The time of mean peak firing rate in untreated control slices on the first day *in vitro* was near ZT7 (ZT7.0 ± 0.3 hr; $n = 7$), and on day 2 *in vitro*, the timing of the peak of the firing rate was near ZT7 for both King's College London (ZT7.1 ± 0.1 hr; $n = 4$) and University of Manchester (ZT7.0 ± 0.2 hr; $n = 6$) rats. Because the timing of the peaks in rat SCN firing rate rhythms was similar in animals from King's College London and the University of Manchester, the data were collapsed into one set (Fig. 1*A*).

The magnitude and direction of phase shifts induced by GRP (10^{-7} M) varied depending on the time of treatment (one-way ANOVA, $F_{(3,21)} = 166.33$, $p < 0.0001$). Compared with untreated, control slices, GRP administered during the subjective day did not significantly alter the time of mean peak firing rate (ZT7.5 ± 0.3 hr; $n = 4$; Dunnett's *post hoc* test, $p > 0.05$) (Fig. 1*B*). However, a 30 min treatment of GRP (10^{-7} M) at ZT13 induced a consistent, nearly 3 hr delay in the time of peak monitored in a single slice over the subsequent days 2 and 3 *in vitro* (see Fig. 3, *top panel*). The time of the mean peak in firing rate on day 2 (ZT10.29 ± 0.14 hr) was significantly different from that seen in control slices (Dunnett's *post hoc*, $p < 0.0001$), with a mean phase delay of −3.2 ± 0.1 hr ($n = 6$) (Fig. 1*C* and see Fig. 6*A*).

Late subjective night (ZT19) GRP treatments (10^{-7} M) resulted in phase shifts of similar magnitude, but in the opposite direction (Fig. 1*D*). The mean peak of firing rate on day 2 (ZT4.3 ± 0.23 hr; $n = 5$) was significantly different from the peak seen in control slices (Dunnett's *post hoc*, $p < 0.0001$). The mean phase advance found after ZT19 treatment was 2.9 ± 0.3 hr ($n = 5$) (see Fig. 6*A*). The phase shift in subsequent circadian cycles was similarly consistent and stable in a single slice, as shown in Figure 3 (*bottom panel*), indicating that GRP-induced phase advances in rat SCN circadian pacemaker phase persist through the third 24 hr cycle *in vitro*.

Application of GRP (10^{-11} to $^{-5}$ M) early in the projected night (ZT13) caused phase delays in the peak in the firing rate rhythm that depended on the dose of GRP (one-way ANOVA, $F_{(5,21)} = 24.49$, $p < 0.00001$). The dose–response curve in Figure 2 demonstrates that a significant phase delay (−1.75 ± 0.4 hr; $n = 3$) was achieved with a concentration as low as 10^{-8} M GRP, but the
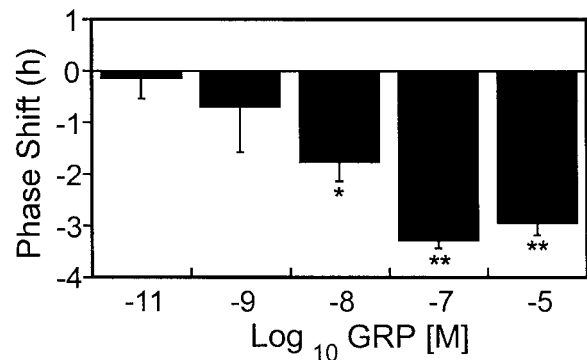

Figure 2. Dose dependency of GRP-induced phase delays at ZT13. Each *bar* represents the mean phase shift (in hour ± SEM) for the dose shown. * Significantly different from time of peak in control slices ($p < 0.05$); ** significantly different from time of peak in control slices ($p < 0.01$).
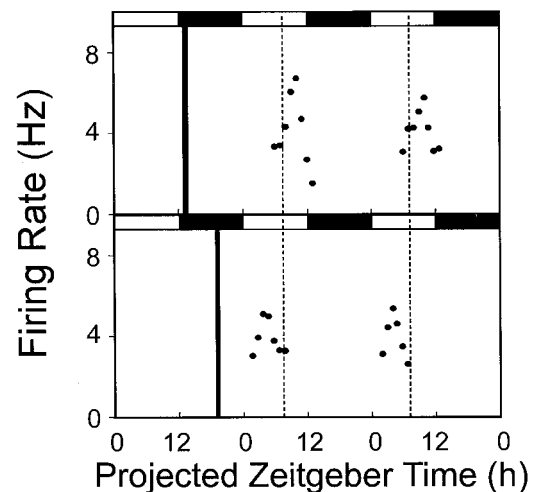

Figure 3. Firing rate rhythms of rat SCN neurons *in vitro* across two projected day–night cycles. *Top panel,* The delay evoked by GRP at ZT13 is similar on days 2 and 3 *in vitro.* *Bottom panel,* The advance evoked by GRP at ZT19 is similar on days 2 and 3 *in vitro.* In each panel, the *solid dots* represent the smoothed running mean firing rate in spikes per second. *Filled* and *unfilled horizontal bars* depict projected night and day portions, respectively, of the projected 48 hr period.

10^{-7} M GRP dose used in our experiments appeared to evoke a maximal response (Fig. 2).

Specific GRP receptor antagonist blocks GRP-induced phase shifts at both early and late subjective night

To determine the receptor-based mechanism mediating the actions of GRP on the rat SCN, the effects of the BB$_2$ receptor antagonist DPDMBE on these phase shifts to GRP were assessed at ZT13 and ZT19. For statistical analysis, the phase shifts to this antagonist in the presence or absence of GRP at ZT13 and ZT19 were compared with the phase-resetting actions of GRP alone (as reported above) (see Fig. 6*A*). Two-way ANOVA showed a nonsignificant main effect of drug, but a significant main effect of time ($F_{(1,29)} = 60.4$, $p < 0.001$) as well as a significant drug × time interaction ($F_{(3,29)} = 103.05$, $p < 0.0001$). *Post hoc* analysis with the Tukey HSD test showed that in comparison to control slices, 45 min application of DPDMBE (10^{-5} M) alone did not significantly alter the time of peak in SCN firing rate at either ZT13 (time of peak = ZT6.98 ± 0.13 hr) or ZT19 (time of peak = ZT7.58 ± 0.22 hr) (Fig. 4, *A* and *C*, respectively). These data confirm that DPDMBE demonstrates no significant GRP receptor agonist properties and does not alter ongoing circadian function at early or late subjective night.

When GRP (10^{-7} M) and DPDMBE (10^{-5} M) were coadministered, after a brief preincubation with the antagonist alone, GRP-
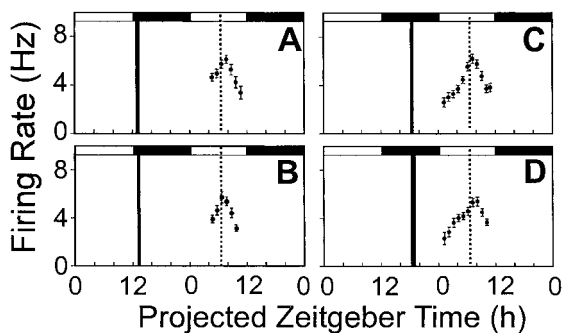
Figure 4. Blockade of GRP-evoked phase delays at ZT13 (_A_) and phase advances at ZT19 (_C_) by the BB₂ receptor antagonist DPDMBE. In comparison to the phase-resetting effects of GRP alone at ZT13 or ZT19 (Fig. 1_C,D_), this antagonist did not alter the time of peak mean firing rate at either ZT13 (_B_) or ZT19 (_D_) but blocked the phase-shifting effects of GRP at these phases. In each panel, the _solid dots_ represent the smoothed running mean firing rate in spikes per second, and the _vertical bars_ are the standard error of that smoothed firing rate mean. _Filled_ and _unfilled horizontal bars_ depict projected night and day portions, respectively, of the projected 48 hr period.
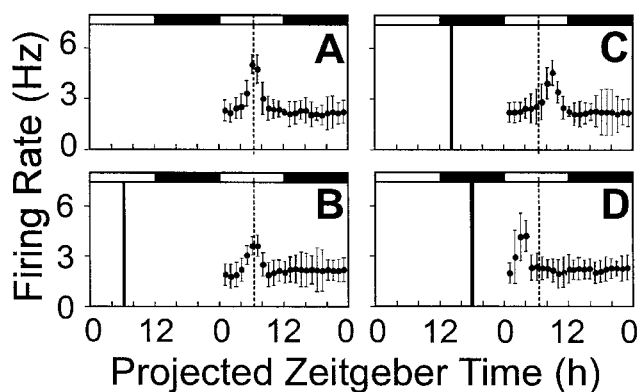
Figure 5. Firing rate rhythms of hamster SCN neurons _in vitro_ across two projected day–night cycles. _A_, The peak in control, untreated slices occurred at projected ZT6.7 on the second day _in vitro_. _B_, Bath-applied GRP (10⁻⁷ M; _filled vertical bar_) at ZT6 failed to significantly reset the time of peak compared with control slices (_vertical dashed line_). _C_, Bath-applied GRP (10⁻⁷ M) at ZT14 significantly phase-delayed the time of peak compared with control slices. _D_, Bath-applied GRP (10⁻⁷ M) at ZT18 phase-advanced the time of peak compared with control slices. In each panel, the _solid dots_ represent the smoothed running mean firing rate in spikes per second, and the _vertical bars_ are the standard error of the smoothed firing rate mean. _Filled_ and _unfilled horizontal bars_ depict projected night and day portions, respectively, of the projected 48 hr period.

induced phase shifts were completely blocked (Tukey HSD, $p < 0.001$). Early subjective night treatment (ZT13) resulted in time of peak at ZT7.31 ± 0.21 hr ($n = 4$), whereas coapplication of GRP and DPDMBE at ZT19 showed a time of peak at ZT 7.44 ± 0.19 hr ($n = 4$) (Fig. 4, _B_ and _D_, respectively). These results demonstrate a selective and phase-specific action of GRP on the rat SCN circadian system.

Electrophysiology: hamsters

GRP phase resets the hamster SCN circadian pacemaker

The action of GRP on the hamster SCN circadian pacemaker was assessed by monitoring the time of peak in the endogenous ensemble firing rate rhythm in SCN neurons. The mean time of peak in untreated control hamster SCN slices on day 2 _in vitro_ was near ZT7 (ZT6.7 ± 0.2 hr; $n = 9$) (Fig. 5_A_). The magnitude and direction of phase shifts induced by bath application of GRP (10⁻⁷ M) varied depending on the time of treatment (one-way ANOVA, $F_{(3,20)} = 161.99$, $p < 0.0001$). Compared with ACSF-treated control slices, GRP administered during the subjective day (ZT6) did not significantly alter the time of peak (ZT6.7 ± 0.1 hr;
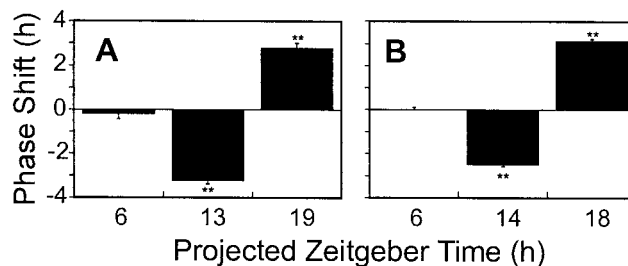

Figure 6. _A_, Phase-shifting effects of GRP (10⁻⁷ M) on firing rate rhythm of rat SCN neurons _in vitro_. Each bar represents the mean ± SEM phase shift (in hours) at that projected zeitgeber time. ** Significantly different from the time of peak seen in control slices ($p < 0.01$). Phase advances are shown as positive values and phase delays as negative values. _B_, Phase-shifting effects of GRP (10⁻⁷ M) on firing rate rhythm of hamster SCN neurons _in vitro_. Each bar represents the mean ± SEM phase shift (in hours) at the projected zeitgeber time. ** Significantly different from the time of peak seen in control slices ($p < 0.01$). Phase advances are shown as positive values and phase delays as negative values.

$n = 5$; Dunnett's _post hoc_, $p > 0.05$) (Fig. 5B). However, at ZT14, GRP (10⁻⁷ M) phase-delayed the timing of the firing rate peak. The mean peak of firing rate on day 2 from slices treated with GRP early in the projected night (ZT9.16 ± 0.13 hr; $n = 5$) was significantly different from that seen in control slices (Dunnett's, $p < 0.0001$), with a mean phase delay of −2.43 ± 0.1 hr (Figs. 5_C_, 6_B_).

Late subjective night (ZT18) GRP treatments (10⁻⁷ M) resulted in phase shifts of similar magnitude, but in the opposite direction (Figs. 5_D_, 6_B_). The mean peak of firing rate on day 2 (ZT3.56 ± 0.24 hr; $n = 5$) was significantly different from the peak seen in control slices (Dunnett's, $p < 0.001$). The mean phase advance found after ZT18 treatment was 3.17 ± 0.3 hr ($n = 5$).

To ascertain whether these phase-resetting actions of GRP on the hamster circadian pacemaker occurred at the level of the SCN, GRP (10⁻⁷ M) or ACSF was applied as microdrops directly onto the SCN at ZT6, ZT14, and ZT18. A two-way ANOVA was used to compare the effects of drug microdrop applications at these projected zeitgeber phases. There was no significant main effect of drug, but there was a significant main effect of projected zeitgeber phase ($F_{(2,24)} = 244.62$, $p < 0.0001$) and a significant drug × zeitgeber phase interaction ($F_{(2,24)} = 188.27$, $p < 0.0001$). The effects of GRP were phase dependent: there was no difference between the effects of ACSF and GRP in slices treated at ZT6, but GRP significantly phase-delayed the peak in the rhythm at ZT14 [time of peak in GRP-treated slices ZT9.2 ± 0.12 hr ($n = 5$) against time of peak in ACSF slices of ZT6.42 ± 0.17 hr ($n = 5$), Tukey HSD, $p < 0.001$], and significantly phase-advanced the peak in the rhythm at ZT18 [time of peak in GRP-treated slices ZT3.74 ± 0.08 hr ($n = 5$) against time of peak in ACSF-treated slices ZT6.42 ± 0.17 hr ($n = 5$), significantly different at $p < 0.001$, Tukey HSD].

To identify the receptor mediating the phase-shifting actions of GRP on the hamster SCN circadian pacemaker, the effects of bath application of the BB₂ receptor antagonist DPDMBE on the effects of GRP were assessed at ZT14 and ZT18. A two-way ANOVA was used to compare the effects of these drugs at these two zeitgeber phases. There was no significant main effect of drug, but there was a significant main effect of zeitgeber phase ($F_{(1,16)} = 170.98$, $p < 0.0001$) and a significant drug × zeitgeber phase interaction ($F_{(3,16)} = 117.98$, $p < 0.0001$). _Post hoc_ analysis with the Tukey HSD test indicated that in comparison with ACSF-treated slices, bath application of DPDMBE (10⁻⁵ M) did not significantly alter the time of peak in hamster SCN firing rate at either phase when GRP shifts the clock (peak in firing rate when applied at ZT14 = ZT6.82 ± 0.22 hr; at ZT18 = ZT6.7 ± 0.15 hr). These data confirm that DPDMBE demonstrates no significant GRP receptor agonist properties in the hamster SCN and does not alter ongoing circadian function at early or late subjective night. When GRP (10⁻⁷ M) and DPDMBE (10⁻⁵ M) were coadministered, after a brief prein-
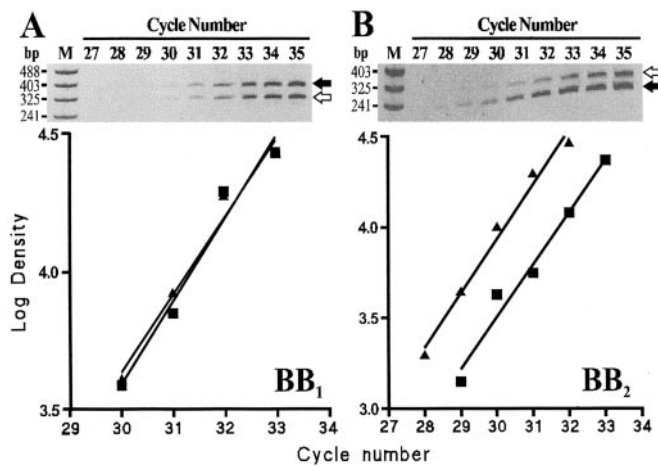
Figure 7. Determination of the efficiency of the PCR for bombesin receptor target and competitor DNAs. cDNA (1/200th) obtained from a single SCN slice was amplified in the same tube as BB_1 (3.6 attogram) or BB_2 (25.8 attogram) competitor in a 40 μl reaction using the cycling conditions described in Materials and Methods. A 2 μl sample was removed from the reaction at the end of the extension phase from cycles 21–38, and the products were separated on an agarose gel, stained, and quantitated by densitometry. The data show (*A*) the increase in BB_1 target (*filled arrow*) and competitor (*open arrow*) and (*B*) BB_2 target (*filled arrow*) and competitor (*open arrow*) with cycle number during the linear (exponential) phase of the reaction. The efficiency of amplification is calculated from the slope of the linear regression line for each product. Efficiencies were as follows: for BB_1 target 92.4% (*filled triangles*), BB_1 competitor 98.3% (*filled squares*), and for BB_2 target 99.3% (*filled triangles*), BB_2 competitor 96.0% (*filled squares*).

cubation with the antagonist alone, GRP-induced phase shifts were completely blocked. Early subjective night (ZT14) treatment with the DPDMBE + GRP combination resulted in time of peak at ZT6.78 ± 0.13 hr ($n = 5$), which was not significantly different from the peak seen in ACSF-treated slices (Tukey HSD, $p > 0.05$) but was significantly different from the time of peak seen in slices treated with GRP alone (Tukey HSD, $p < 0.0001$). Slices treated with DPDMBE and GRP at ZT18 showed a time of peak at ZT6.7 ± 0.15 hr ($n = 5$), which was not significantly different from the time of peak seen in ACSF-treated control slices (Tukey HSD, $p > 0.05$) but was significantly different from time of peak seen in slices treated with GRP alone at this time of the projected night (Tukey HSD, $p < 0.001$). These results demonstrate that both the phase-delaying and phase-advancing actions of GRP are blocked by the BB_2 receptor antagonist DPDMBE, indicating a phase-specific and receptor-mediated action of GRP on the hamster SCN circadian pacemaker.

RT-PCR: quantitation of bombesin receptor subtype expression in SCN

BB_1 receptor

A single PCR product of the expected size (388 bp) was amplified from 35 of the 36 SCN cDNA samples using the common sense primer and the BB_1 receptor specific antisense primer. Sequencing showed that this product was derived from authentic BB_1 receptor mRNA. No PCR products were amplified from SCN mRNA samples when the RT step was omitted (data not shown). A competitor DNA (316 bp) having the same primer annealing sequences as BB_1 cDNA was prepared by low-stringency PCR and was shown to amplify with very similar efficiency (Fig. 7A) (92.4% for BB_1 target and 98.3% for BB_1 competitor), allowing it to be used for quantitative competitive PCR. Competitive PCR, using a fixed small amount of target cDNA (1/200th of the SCN sample) and a twofold dilution series of competitor gave two PCR products as shown in Figure 8A (*top*). For each SCN sample a plot of the log ratio of BB_1 target/competitor against concentration of competitor initially added to the reaction indicated a linear relationship (Fig. 8B, *bottom*). These linear regression lines were significant ($p < 0.05$)
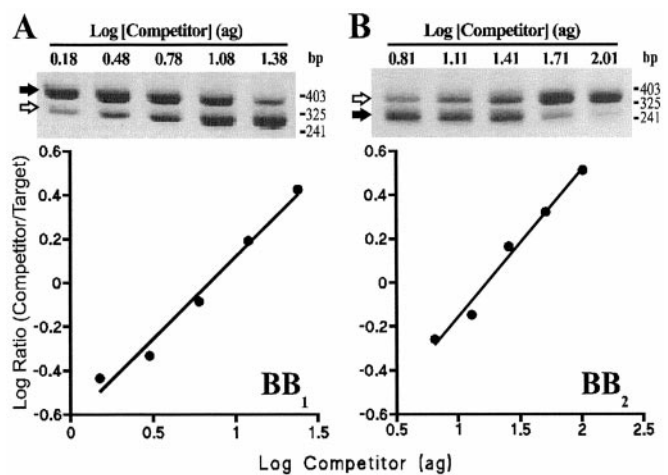

Figure 8. An example of competitive RT-PCR for the BB_1 (*A*) and the BB_2 (*B*) receptor. *Top*, Gel images showing authentic BB_1 and BB_2 receptor target (*filled arrows*) and competitor (*open arrows*). The amount of competitor (attogram) added at the start of the reaction is indicated above each lane. Molecular weight markers are indicated (*Hpa*II digest of pBluescript SK+). *Bottom*, The density of target and competitor bands on the gels (arbitrary units) were measured and corrected for the difference in size, and the log ratio was calculated and plotted as a function of the amount of competitor DNA included at the start of the PCR reaction. From the regression lines shown, the amount of BB_1 and BB_2 receptor cDNA present in the reaction was calculated (i.e., when log ratio target/competitor = 0). For BB_1 $r^2 = 0.981$, $p = 0.001$; for BB_2 $r^2 = 0.983$, $p = 0.0009$.
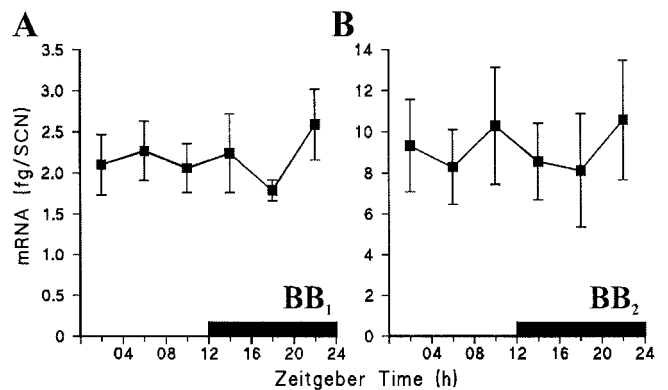

Figure 9. Daily pattern of expression of BB_1 (*A*) and BB_2 (*B*) receptor mRNA in the rat SCN. Values are the mean ± SEM femtogram of mRNA/SCN of six rats at each time point. *Solid bar* indicates the dark period (7 P.M.-7 A.M.).

for all SCN cDNA samples (range r^2 0.807–0.998). Figure 9A shows the variation in SCN BB_1 receptor mRNA expression across the light/dark cycle. One-way ANOVA indicated no significant daily variation in the amount of SCN BB_1 receptor mRNA ($F_{(5,28)} = 0.38$, $p > 0.05$).

BB_2 receptor

For the BB_2 receptor, a single PCR product of the expected size (298 bp) was amplified from 35 of the 36 SCN cDNA samples. Sequencing confirmed that it derived from authentic BB_2 receptor mRNA. No PCR products were amplified from SCN mRNA samples when the RT step was omitted (data not shown). A BB_2 competitor DNA (363 bp) was prepared and shown to amplify with very similar efficiency to BB_2 target (Fig. 7B) (99.3% for BB_2 target and 96.0% for BB_2 competitor). When a fixed amount of SCN cDNA (1/200th of the SCN sample) was amplified with competitor (twofold dilution series), two PCR products were generated (Fig. 8B, *top*). The log of the ratio of BB_2 target/competitor was significantly related to the concentration of competitor initially added to the reaction for all SCN samples (Fig. 8B, *bottom*) ($p < 0.05$, range

r^2 0.834–0.999). There was no significant daily variation in the amount of SCN BB_2 receptor mRNA expressed across the light/dark cycle (one-way ANOVA, $F_{(5,28)} = 0.18$, $p > 0.05$) (Fig. 9*B*).

DISCUSSION

The timing in the peaks of the firing rate rhythms measured under control conditions in the SCNs of Wistar rats and Syrian hamsters (~ZT7.0 and ~ZT6.7, respectively) are similar to those previously reported for these species (Gillette, 1986; Biello et al., 1997). In both species, GRP (10^{-7} M) given during the middle of the subjective day did not alter the timing of the electrical activity rhythm. In contrast, 10^{-7} M GRP applied during the early portions of the subjective night significantly phase-delayed (~3.2 hr in rat and ~2.5 hr hamster) the time of peak and significantly phase-advanced (~2.9 hr in rats and ~3.1 hr in hamsters) the time of peak of this SCN cellular rhythm when given late in the subjective night. In rats, GRP dose-dependently phase-delayed the firing rate rhythm, with small but significant phase delays (~1.75 hr) evoked by the 10^{-8} M concentration. This shows that GRP in the nanomolar range can alter the timing of the circadian pacemaker in the rat SCN. Furthermore, in both species, the BB_2 receptor antagonist DPDMBE blocked the phase-shifting effects of GRP, indicating that this resetting action of GRP is mediated through this receptor subtype. Overall, this temporal pattern of phase resetting by GRP strongly resembles the phase–response curves for light pulses on hamster behavioral rhythms (Daan and Pittendrigh, 1976; Takahashi et al., 1984) as well as glutamate on rodent SCN firing rate rhythms *in vitro* (Ding et al., 1994; Biello et al., 1997).

The phase-shifting actions of GRP on the rodent circadian pacemaker *in vitro* appear to occur at the level of the SCN because microdrop application of GRP directly onto the hamster SCN altered the timing of the firing rate rhythm in the same direction and at the same phases as bath applications of GRP. This is also concordant with previous *in vivo* studies showing that GRP microinjected within 600 μm of hamster SCN phase-dependently phase-resets wheel-running rhythms, whereas microinjections into hypothalamic regions beyond 600 μm of the SCN were ineffective (Piggins et al., 1995). Although Albers and colleagues (1991, 1995) found that *in vivo*, GRP needed to be coapplied with other peptides to significantly reset hamster behavioral rhythms, our present results demonstrate that GRP alone can evoke large phase shifts in the hamster and rat SCN circadian pacemaker. Whether GRP acts directly on pacemaker neurons or indirectly via interneurons remains to be determined.

Using an established competitive quantitative RT-PCR protocol (Sugden et al., 1999), we detected and measured the level of expression of BB_1 and BB_2 receptor genes in the rat SCN across the diurnal cycle. The BB_2 receptor was expressed in greater amounts than that of the BB_1 receptor. Neither BB_1 nor BB_2 receptor mRNA was found to vary over the day–night cycle, indicating that at this level of analysis, diurnal variation in the expression of these receptors is unlikely to underlie the phase-dependent actions of GRP on the SCN circadian pacemaker.

The detection of BB_2 receptor gene expression in the rat SCN is in broad agreement with previously published radioligand and *in situ* hybridization reports showing heavy expression of radiolabeled GRP and BB_2 receptor mRNA in the rat SCN (Zarbin et al., 1985; Battey and Wada, 1991). However, our measurement of low levels of expression of BB_1 receptor mRNA by RT-PCR contrasts with the results of previous radioreceptor and *in situ* hybridization studies that failed to find significant binding of radiolabeled BB_1 ligands or expression of BB_1 receptor mRNA in the rat SCN, respectively (Ladenheim et al., 1990, 1992, 1993; Wada et al., 1991). This disparity is presumably attributable to the greater sensitivity of the competitive quantitative RT-PCR techniques over radiolabeling and *in situ* hybridization methodologies.

The observation that both BB_1 and BB_2 receptor mRNAs are expressed in the rodent SCN is consistent with findings from previous *in vitro* neurophysiological studies (Piggins et al., 1994; Pinnock et al., 1994). In these investigations, it was found that

selective BB_2 ligands (GRP and $GRP_{18–27}$) and the BB_1 ligand (neuromedin B) potently excited rodent SCN neurons. This suggests that BB_1 and BB_2 receptors are functionally expressed in the rodent SCN. Further experiments with selective agonists and antagonists to the BB_1 receptor subtype are required to elucidate the function of these receptors in the SCN and their possible contribution to the phase-resetting effects of GRP.

The pattern of phase shifting evoked by GRP *in vitro* strongly resembles its *in vivo* phase-dependent action on hamster wheel-running rhythms. In these studies, it was found that microinjections of GRP into the SCN region of hamsters free-running in constant conditions evoked large phase delays (~1 hr) on hamster wheel-running rhythms when administered early in the subjective night and modest phase advances (~0.5 hr) when given late in the subjective night. In contrast, similar microinjections during the middle portions of the subjective day failed to alter the phase of wheel running (Piggins et al., 1995). The only notable difference between the *in vivo* and *in vitro* effects of GRP is that the magnitude of the shifts was greater *in vitro*. The reasons for this difference are unknown but are presumably attributable to the absence of modulating inputs to the SCN *in vitro*. Nonetheless, the results demonstrate a remarkable concordance in the phase sensitivity and direction of shifts induced by GRP on the rodent SCN, both between species and across experimental settings.

Our finding that the BB_2 receptor antagonist DPDMBE did not alter the timing of the peak in firing rate suggests that GRP does not play a tonic role in the production of the circadian rhythm in the rodent SCN neuronal firing rate. This contention is supported by results from studies indicating that under constant conditions there is no endogenous rhythm in the production of GRP in the rat SCN and that a rhythm in GRP levels only becomes apparent under the influence of a light/dark cycle (Shinohara et al., 1993; Okamura and Ibata, 1994). It was previously demonstrated that the BB_2 receptor antagonist BIM 26226 did not have any effect on hamster running-wheel activity rhythms when microinjected into the hamster SCN early in the subjective night (Piggins et al., 1995). Taken together, these findings support the hypothesis that although GRP may be involved in the process of photic entrainment, it does not appear to play a functional role in the free-running SCN pacemaker.

Both the results presented here and those reported previously from *in vivo* experiments (Albers et al., 1991, 1995; Piggins et al., 1995) demonstrate a high degree of phase dependency in the effects of GRP in resetting the circadian pacemaker. Because GRP levels do not spontaneously oscillate and because the RT-PCR results presented here indicate that levels of both BB_1 and BB_2 receptor mRNA do not show diurnal fluctuation, the basis for the phase dependency of the GRP effects remains obscure. One possibility is that glutamate from RHT terminals excites GRP-synthesizing neurons, causing the release of GRP onto adjacent SCN neurons, which in turn can modulate the activational actions of glutamate on other SCN neurons. Alternatively, GRP may be released from RHT terminals and evokes the further release of GRP from retinorecipient neurons (McKillop et al., 1988).

The BB_2 receptor is a classic G-protein-linked, seven transmembrane domain protein the activation of which leads to stimulation of intracellular signaling cascades involving, among others, protein kinase A, protein kinase C, and mitogen-activated protein kinases (Hansson, 1994; Kroog et al., 1995). These signaling molecules themselves have been implicated in phase-dependent phase-shifting effects of other neurochemicals on the SCN (Prosser et al., 1994; McArthur et al., 1997; Obrietan et al., 1998). Circadian variations in the levels of intracellular signaling factors that are activated after GRP binding to the BB_2 receptor may underlie the phase dependency of the phase-shifting effects of GRP.

In conclusion, GRP phase-dependently phase-resets the electrical activity rhythm of rodent SCN neurons *in vitro*. These effects showed dose dependency and were blocked by pretreatment with the BB_2 receptor antagonist DPDMBE. Using a quantitative competitive RT-PCR protocol, expression of both BB_1 and BB_2 recep-

tor mRNAs was detectable within rat SCN, with the BB_2 receptor mRNA more heavily expressed than BB_1 receptor mRNA. Significant diurnal variation in the expression of these transcripts was not apparent, suggesting that the circadian gating of the effects of GRP on the rat SCN occurs at a level downstream of the receptor. These data show that GRP potently resets the rodent SCN *in vitro* in a manner resembling the effects of light on rodent behavioral rhythms. These results raise the possibility that GRP and GRP receptors play a role in the photic entrainment of the SCN circadian pacemaker. Further studies with BB_2 receptor antagonists are required to determine whether this receptor plays a physiological role in mediating the effects of light on the rodent SCN.

REFERENCES

Aïoun J, Chambille I, Peytevin J, Martinet L (1998) Neurons containing gastrin-releasing peptide and vasoactive intestinal polypeptide are involved in the reception of the photic signal in the suprachiasmatic nucleus of the Syrian hamster: an immunocytochemical ultrastructural study. Cell Tissue Res 291:239–253.

Albers HE, Liou S-Y, Stopa EG, Zoeller RT (1991) Interaction of colocalized neuropeptides: functional significance in the circadian timing system. J Neurosci 11:846–851.

Albers HE, Gillespie CF, Babagbemi TO, Huhman KL (1995) Analysis of the phase shifting effects of gastrin releasing peptide when microinjected into the suprachiasmatic nucleus. Neurosci Lett 191:63–66.

Battey J, Wada E (1991) Two distinct receptor subtypes for mammalian bombesin-like peptides. Trends Neurosci 14:524–528.

Biello SM, Golombek DA, Harrington ME (1997) Neuropeptide Y and glutamate block each other's phase shifts in the suprachiasmatic nucleus *in vitro*. Neuroscience 77:1049–1058.

Colwell CS, Menaker M (1996) Regulation of circadian rhythms by excitatory amino acids. In: Excitatory amino acids: their roles in neuroendocrine function (Brann DW, Mahesh VB, eds), pp 223–252. Boca Raton, FL: CRC.

Daan S, Pittendrigh CS (1976) A functional analysis of circadian pacemakers in nocturnal rodents: II. The variability of phase response curves. J Comp Physiol 106:253–266.

D'Aquila RT, Bechtel LJ, Videler JA, Eron JJ, Gorczyca P, Kaplan JC (1991) Maximizing sensitivity and specificity of PCR by preamplification heating. Nucleic Acids Res 19:37–49.

Devereux J, Haberli P, Smithies A (1984) A comprehensive set of sequence analysis programs for VAX and CONVEX systems. Nucleic Acids Res 12:387–394.

Ding JM, Chen D, Weber ET, Faiman LE, Rea MA, Gillette MU (1994) Resetting the biological clock: mediation of nocturnal circadian shifts by glutamate and NO. Science 266:1713–1717.

Earnest DJ, DiGiorgio S, Olschowka JA (1993) Light induces expression of fos-related proteins within gastrin-releasing peptide neurons in the rat suprachiasmatic nucleus. Brain Res 627:205–209.

Ebling FJP (1996) The role of glutamate in the photic regulation of the suprachiasmatic nucleus. Prog Neurobiol 50:109–132.

Gillette MU (1986) The suprachiasmatic nuclei: circadian phase-shifts induced at the time of hypothalamic slice preparation are preserved *in vitro*. Brain Res 379:176–181.

Hansson A (1994) Map kinase activation in Swiss 3T3 cells stimulated with gastrin-releasing peptide is associated with increased phosphorylation of a 78,000 M(r) protein immunoprecipitated by anti-raf kinase anti-serum. Cell Signal 4:423–431.

Harrington ME (1997) The ventral lateral geniculate nucleus and the intergeniculate leaflet: interrelated structures in the visual and circadian systems. Neurosci Biobehav Rev 21:705–729.

Kroog GS, Jensen RT, Battey JF (1995) Mammalian bombesin receptors. Med Res Rev 15:389–417.

Ladenheim EE, Jensen RT, Mantey SA, McHugh PR, Moran TH (1990) Receptor heterogeneity for bombesin-like peptides in the rat central nervous system. Brain Res 537:233–240.

Ladenheim EE, Jensen RT, Mantey SA, Moran TH (1992) Distinct distributions of two bombesin receptor subtypes in the rat central nervous system. Brain Res 593:168–178.

Ladenheim EE, Jensen RT, Mantey SA, Taylor JE, Coy DH, Moran TH (1993) Bombesin receptor antagonists differentiate receptor subtypes in rat brain. Eur J Pharmacol 235:121–125.

McArthur AJ, Hunt AE, Gillette MU (1997) Melatonin action and signal

transduction in the rat suprachiasmatic circadian clock: activation of protein kinase C at dusk and dawn. Endocrinology 138:627–634.

McKillop JM, Fow WL, Johnston CF, Shaw C, Murphy RF, Buchanan KD (1988) Gastrin-releasing peptide (GRP) immunoreactivity in the rat retina: a radioimmunoassay, immunohistochemical and chromatographic study. Brain Res 447:239–245.

Meijer JH, Rietveld WJ (1989) Neurophysiology of the suprachiasmatic circadian pacemaker in rodents. Physiol Rev 69:671–707.

Mikkelsen JD, Larsen PJ, O'Hare MMT, Wiegand SJ (1991) Gastrin releasing peptide in the rat suprachiasmatic nucleus: an immunohistochemical, chromatographic, and radioimmunological study. Neuroscience 40:55–66.

Obrietan K, Imprey S, Storm DR (1998) Light and circadian rhythmicity regulate MAP kinase activation in the suprachiasmatic nuclei. Nat Neurosci 1:693–700.

Okamura H, Ibata Y (1994) GRP immunoreactivity shows a day-night difference in the suprachiasmatic nucleus soma and efferent fibers: comparison to VIP immunoreactivity. Neurosci Lett 181:165–168.

Panula P, Yang H-YT, Costa E (1984) Comparative distribution of bombesin/grp- and substance P-like immunoreactivities in rat hypothalamus. J Comp Neurol 224:606–617.

Piggins HD, Rusak B (1999) Intercellular interactions and the physiology of circadian rhythms in mammals. In: Handbook of behavioral state control: cellular and molecular mechanisms (Lydic R, Baghdoyan HA, eds), pp 31–44. Boca Raton, FL: CRC.

Piggins HD, Cutler DJ, Rusak B (1994) Effects of ionophoretically applied bombesin-like peptides on hamster suprachiasmatic nucleus neurons *in vitro*. Eur J Pharmacol 271:413–419.

Piggins HD, Antle M, Rusak B (1995) Neuropeptides phase shift the mammalian circadian pacemaker. J Neurosci 15:5612–5622.

Pinnock RD, Reynolds T, Woodruff GN (1994) Different types of bombesin receptors on neurons in the dorsal raphe nucleus and rostral hypothalamus in rat brain slices *in vitro*. Brain Res 653:119–124.

Prosser RA, Heller HC, Miller JD (1994) Serotonergic phase advances of the mammalian circadian clock involve protein kinase A and K+ channel opening. Brain Res 644:67–73.

Ralph MR, Foster RG, Davis FC, Menaker M (1990) Transplanted suprachiasmatic nucleus determines circadian period. Science 247:975–978.

Romijn HJ, Sluiter AA, Pool CW, Wortel J, Buijs RM (1996) Differences in colocalization between Fos and PHI, GRP, VIP and VP in neurons of the rat suprachiasmatic nucleus after a light stimulus during the phase delay versus phase advance period of the night. J Comp Neurol 372:1–8.

Roth KA, Weber E, Barchas JD (1982) Distribution of gastrin releasing peptide-bombesin-like immunostaining in rat brain. Brain Res 251:277–282.

Shinohara K, Tominaga K, Isobe Y, Inouye ST (1993) Photic regulation of the peptides located in the ventrolateral subdivision of the suprachiasmatic nucleus of the rat: daily variations of vasoactive intestinal polypeptide, gastrin-releasing peptide, and neuropeptide Y. J Neurosci 13:793–799.

Sugden D, McArthur AJ, Ajpru S, Duniec K, Piggins HD (1999) Expression of mt1 melatonin receptor subtype mRNA in the entrained rat suprachiasmatic nucleus: a quantitative RT-PCR study across the diurnal cycle. Mol Brain Res 72:176–182.

Takahashi JS, DeCoursey PJ, Bauman L, Menaker M (1984) Spectral sensitivity of a novel photoreceptive system mediating entrainment of mammalian circadian rhythms. Nature 308:186–188.

Tanaka M, Hayashi S, Tamada Y, Ikeda T, Hisa Y, Takamatsu T, Ibata Y (1997) Direct retinal projections to GRP neurons in the suprachiasmatic nucleus of the rat. NeuroReport 8:2187–2191.

Uberla K, Platzer C, Diamantstein T, Blankenstein T (1991) Generation of competitor DNA fragments for quantitative PCR. PCR Methods Appl 1:136–139.

Wada E, Way J, Shapiro H, Kusano K, Lebacq-Verheyden AM, Jensen RT, Battey J (1991) cDNA cloning, characterization, and brain region-specific expression of a neuromedin B preferring bombesin receptor. J Neurosci 10:2917–2930.

Zarbin MA, Kuhar MJ, O'Donohue TL, Wolf SS, Moody TW (1985) Autoradiographic localization of (125-I-Tyr4)bombesin binding sites in the rat brain. J Neurosci 5:429–437.

Zoeller RT, Broyles B, Earley J, Anderson ER, Albers HE (1992) Cellular levels of messenger ribonucleic acids encoding vasoactive intestinal polypeptide and gastrin-releasing peptide in neurons of the suprachiasmatic nucleus exhibit distinct 24-hour rhythms. J Neuroendocrinol 4:119–124.